ARMY RESEARCH LABORATORY

Low Cost, High Performance Avalanche Photodiodes for Enabling High Sensitivity Bio-fluorescence Detection (First Year of a Two-year Program)

by Anand V. Sampath and Michael Wraback

ARL-TR-5528 **April 2011**

NOTICES

Disclaimers

The findings in this report are not to be construed as an official Department of the Army position unless so designated by other authorized documents.

Citation of manufacturer's or trade names does not constitute an official endorsement or approval of the use thereof.

Destroy this report when it is no longer needed. Do not return it to the originator.

Army Research Laboratory
Adelphi, MD 20783-1197

ARL-TR-5528 **April 2011**

Low Cost, High Performance Avalanche Photodiodes for Enabling High Sensitivity Bio-fluorescence Detection (First Year of a Two-year Program)

Anand V. Sampath and Michael Wraback
Sensors and Electron Devices Directorate, ARL

REPORT DOCUMENTATION PAGE	Form Approved OMB No. 0704-0188

1. REPORT DATE *(DD-MM-YYYY)*	2. REPORT TYPE	3. DATES COVERED (From - To)
April 2011	DRI	October 2009 to October 2010

4. TITLE AND SUBTITLE
Low Cost, High Performance Avalanche Photodiodes for Enabling High Sensitivity Bio-fluorescence Detection (First Year of a Two-year Program)

5a. CONTRACT NUMBER

5b. GRANT NUMBER

5c. PROGRAM ELEMENT NUMBER

6. AUTHOR(S)
Anand V. Sampath and Michael Wraback

5d. PROJECT NUMBER

5e. TASK NUMBER

5f. WORK UNIT NUMBER

7. PERFORMING ORGANIZATION NAME(S) AND ADDRESS(ES)
U.S. Army Research Laboratory
ATTN: RDRL-SEE-M
2800 Powder Mill Road
Adelphi MD 20783-1197

8. PERFORMING ORGANIZATION REPORT NUMBER
ARL-MR-5528

9. SPONSORING/MONITORING AGENCY NAME(S) AND ADDRESS(ES)

10. SPONSOR/MONITOR'S ACRONYM(S)

11. SPONSOR/MONITOR'S REPORT NUMBER(S)

12. DISTRIBUTION/AVAILABILITY STATEMENT
Approved for public release; distribution unlimited.

13. SUPPLEMENTARY NOTES

14. ABSTRACT
In this report we discuss the modeling, fabrication, and characterization of novel ultraviolet separate absorption and multiplication avalanche photodiodes (SAM-APDs) employing a gallium nitride (GaN) absorption region and a 4H-silicon carbide (SiC) multiplication region. We demonstrate the importance of polarization induced interface charge on the electric field distribution within the quantum efficiency of this device. In addition, we show that the total interface charge can be controlled for optimal detector performance through the use on an interface charge control layer. Finally, we report on the fabrication and testing of GaN/SiC SAM-APDS grown by plasma-assisted molecular beam epitaxy.

15. SUBJECT TERMS
Ultraviolet detectors, avalanche photodiodes, GaN, SiC

16. SECURITY CLASSIFICATION OF:			17. LIMITATION OF ABSTRACT	18. NUMBER OF PAGES	19a. NAME OF RESPONSIBLE PERSON
a. REPORT	b. ABSTRACT	c. THIS PAGE			Anand V. Sampath
Unclassified	Unclassified	Unclassified	UU	24	19b. TELEPHONE NUMBER (*Include area code*) (301) 394-0104

Contents

List of Figures

Acknowledgments

We gratefully acknowledge the support of Dr. Paul Shen (RDRL-SEE-M) in modeling the effects of interface polarization charge on III-Nitride/silicon carbide (SiC) avalanche photodiodes (APDs) and Mr. Ryan Enck (RDRL-SEE-M) for the growth and characterization of some of these structures. We also acknowledge Professor J. Campbell, University of Virginia, and his doctoral students Mr. Q. Zhou and Ms. D. McIntosh for technical discussion as well as the fabrication and characterization of these devices.

INTENTIONALLY LEFT BLANK.

1. Objective

Ultraviolet (UV) light induced fluorescence-based biosensors, like the next generation joint U.S./UK Low Cost Bioagent Sensor (LCBAS) under development by Edgewood Chemical and Biological Center (ECBC), are designed as low-cost, compact, robust, and energy efficient sensors to be deployed as a network of point sensors providing real-time early warning to troops on the battlefield. A major problem for the fielding of such sensors is use of photomultiplier tube (PMT) detectors, which are expensive and fragile, and operate at high voltages. Possible alternatives, including UV-enhanced silicon (Si) avalanche photodiodes (APDs) or silicon carbide (SiC) APDs, have either excessive dark current, poor detectivity, or non-optimal spectral range. The objective of this Director's Research Initiative is to fabricate low dark current, high quantum efficiency, low noise, semiconductor-based single photon counting detectors in the 300 to 550 nm spectral range to replace PMTs currently employed in bio-fluorescence detection. These novel detectors are separate absorption and multiplication avalanche photodiodes (SAM-APDs) that combine high quantum efficiency gallium nitride (GaN) (300 to 360 nm) and indium gallium nitride (InGaN) (360 to 550 nm) absorbers with the proven low dark current, low noise SiC multiplication regions inherent to photon counting Geiger mode SiC APDs to achieve performance comparable to PMTs while reducing cost and improving deployability.

2. Approach

We have fabricated SAM-APDs that employ high quantum efficiency and spectrally tunable (In)GaN in the absorption region and proven low noise, low dark current SiC in the multiplication region. The basic device is a top illuminated structure designed for pure hole injection and multiplication consisting of a heavily doped p+-SiC layer, followed by a lightly doped ν-SiC multiplication layer, an unintentionally doped ν- (In)GaN absorber, and a thin, heavily doped, n^+-GaN layer, as shown in figure 1. The (In)GaN layers are deposited by plasma-assisted molecular beam epitaxy on commercially purchased SiC epilayers/substrates. This design has significant advantages that include the possibility of having high quantum efficiency (QE) over a widely tunable spectral range from the visible to the deep UV by modifying the composition of the direct bandgap III-Nitride absorption region, as well as low dark current and high gain associated with the high quality SiC multiplication region. In addition, this device structure benefits from the formation of a type II heterojunction between the III-Nitride and 4H SiC layers with both the conduction and valence band energies of the GaN below those of the SiC and conduction band and valence band offsets that are between –0.6 and –0.9 eV and 0.7 and 1 eV, respectively (*1*). This band alignment promotes hole injection and inhibits electron injection from GaN into SiC, enabling single carrier injection of the photo-generated holes in the

absorbing region into the SiC multiplication layer that is optimal since the hole ionization coefficient of SiC is much greater than that of the electron. As a result, these devices may have lower noise than SiC APDs.

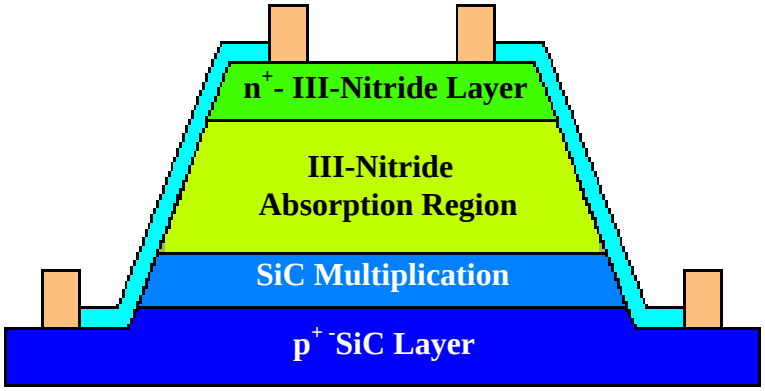

Figure 1. Device structure of a III-Nitride/SiC APD.

However, unlike traditional heterojunction SAM-APDs such as indium gallium arsenide (InGaAs)/indium phosphide (InP) telecommunications devices, these detectors employ polar materials, with the SiC multiplication region having smaller spontaneous polarization than the III-Nitride absorption region. The positive polarization charge expected to form at the hetero-interface between (In)GaN and SiC for III-face growth can achieve an optimal electric field profile in this device, consisting of a high field in the multiplication region of the structure desirable for high gain and a low field within the absorption region. However, insufficient or excessive charge can lead to a suboptimal field distribution and a concomitant reduce QE. As a result, an additional method for controlling the density of interface charge is desirable.

Furthermore, InGaAs/InP APDs benefit from lattice matching of these materials as well as the ability to epitaxially grow the InP multiplication region and InGaAs absorption region directly on an InP substrate without interruption at the hetero-interface. In this manner, the formation of deleterious defects at the hetero-interface can be prevented. In contrast, GaN has a 3.4% lattice mismatch with 4H-SiC that increases with InN mole fraction, resulting in the formation of threading dislocations that can act as leakage paths that increase dark current and prevent avalanche breakdown. While various heteroepitaxial buffer schemes have been developed for the growth of III-Nitrides on SiC, these approaches must be modified or preferably avoided since the SiC region is not simply a substrate and the success of these devices hinges upon the efficient collection of photo-generated holes in the SiC multiplication region.

In the first year of this program, we have focused on developing the growth on GaN directly upon SiC multiplication structures for realizing APDs with low dark current. In addition, we have investigated the role of polarization-induced charge on the performance of GaN/SiC SAM-APDs through calculations of the electric field profile in these devices and developed new

techniques for controlling the density of interface charge to achieve optimal detector performance. Lastly, prototype InGaN/SiC SAM-APDs were developed to extend these devices into the visible spectrum.

3. Results

3.1 Modeling

The relationship between the electric field at the hetero-interface between GaN and SiC and the polarization-induced charge is given by Gauss' Law, which can be expressed for this case as

$$\varepsilon_{SiC} E_{SiC} = \varepsilon_{GaN} E_{GaN} + \sigma_n \tag{1}$$

where E_{SiC}, E_{GaN}, ε_{SiC}, and ε_{GaN} are the electric field and dielectric constant in the SiC multiplication, and GaN absorption regions, respectively, and σ_n is the net interface charge density. As we will demonstrate, σ_n strongly impacts the electric field distribution in this device, and therefore, detector performance. Consider the case of the detector structure shown in figure 1 under large reverse bias V_b just short of avalanche breakdown. Neglecting the contributions from the band offset between GaN and SiC and the space charge in the p+ and n+ regions, the applied voltage may be expressed as

$$E_{SiC} d_{SiC} + E_{GaN} d_{GaN} = V_b \tag{2}$$

where d_{SiC} and d_{GaN} are the thickness of the depletion region in the n^- SiC and n^- GaN layers, respectively.

Equations 1 and 2 can be solved for the distribution of the electric field in the SiC multiplication region and the GaN absorption region, which can be expressed as

$$\begin{cases} E_{GaN} = \dfrac{\varepsilon_{SiC} V_b - \sigma_n d_{SiC}}{\varepsilon_{GaN} d_{SiC} + \varepsilon_{SiC} d_{GaN}} \\ E_{SiC} = \dfrac{\varepsilon_{GaN} V_b + \sigma_n d_{GaN}}{\varepsilon_{GaN} d_{SiC} + \varepsilon_{SiC} d_{GaN}} \end{cases} \tag{3}$$

However, these expressions are only valid for the case where

$$V_b > \frac{\sigma_n}{\varepsilon_{SiC}} d_{SiC} \tag{4}$$

When the electric field can punch through into the GaN absorption region, as illustrated in the band diagram in figure 2 (left). For the circumstances where equation 4 is not satisfied, a two-dimensional electron gas (2DEG) forms in the GaN at the hetero-interface to offset σ_n as shown in figure 2 (right) and the electric field in the GaN and SiC regions are instead given by

$$\begin{cases} E_{GaN} = 0 \\ E_{SiC} = \dfrac{V_b}{d_{SiC}} \end{cases} \tag{5}$$

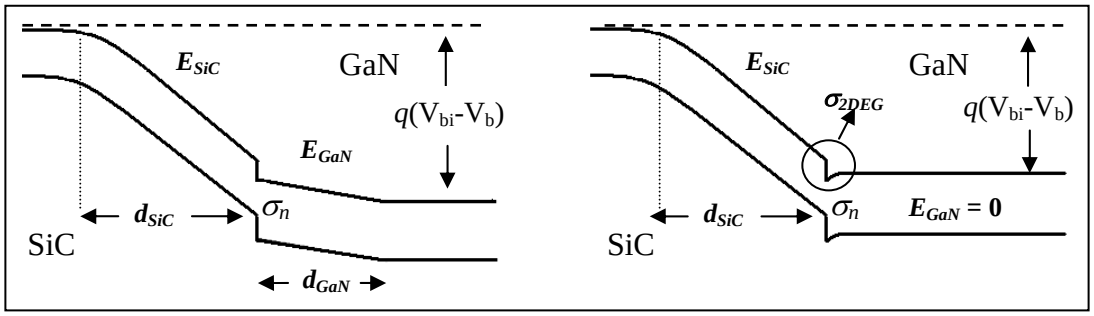

Figure 2. Band diagram of a GaN/SiC APD under reverse bias, with the electric field either showing punch-through into the GaN absorption region (left) or confined in the SiC multiplication region (right) due to the presence of polarization induced charge σ at the interface.

Figure 3 shows the calculated electric field in the GaN absorption and SiC multiplication regions as a function of applied bias for a number of net interface charge densities. At small reverse bias, the electric field is confined entirely within the SiC layer. When the applied bias satisfies the condition in equation 4, punch-though occurs and $E_{GaN} \neq 0$. It is clear from figure 3 that increasing interface charge increases the bias required to achieve punch-through. However the critical field in the SiC multiplication region (E_{SiC}^{cr}), beyond which avalanche breakdown occurs, places an upper limit on the applied reverse bias. As a result, excessive interface charge makes it impossible to extend the electric field to the GaN region prior to avalanche breakdown within the SiC multiplication region, thus reducing the QE of the detector by limiting charge collection to a primarily diffusion mechanism in the absorption region. In contrast, insufficient charge will lead to excessive electric field in the absorber region, resulting in increased injection of background carriers from the absorption region into the multiplication region, and therefore, higher dark current. For an optimized device, the electric field in the SiC multiplication region should approach but not exceed E_{SiC}^{cr}, while the electric field in the GaN absorption region should be non-zero, but less than the breakdown field for GaN (E_{GaN}^{br}), i.e.,

$$\begin{cases} 0 < E_{GaN} < E_{GaN}^{br} \\ E_{SiC} \approx E_{SiC}^{cr} \end{cases} \tag{6}$$

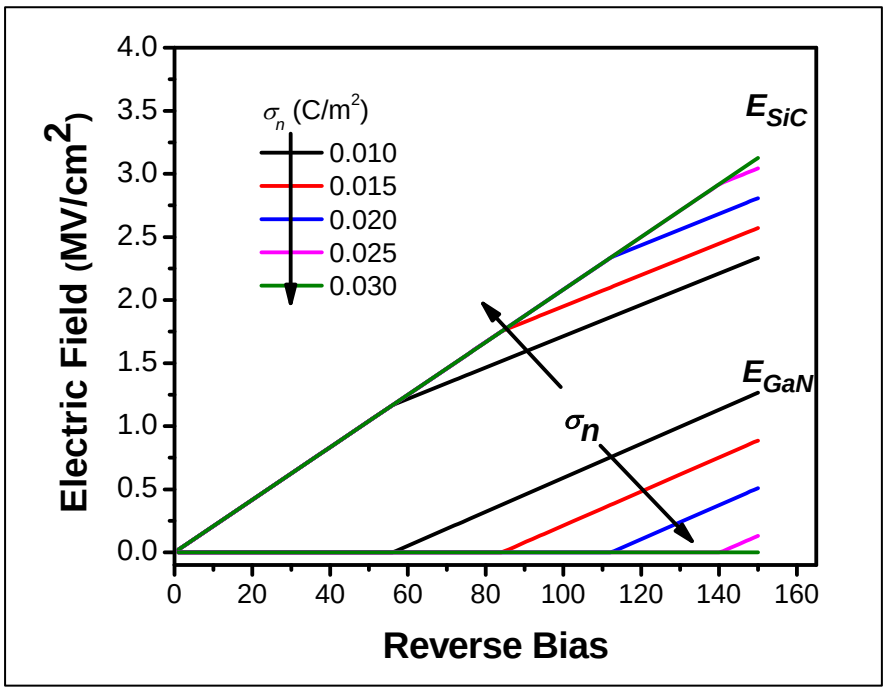

Figure 3. Calculation of the electric field distribution in the GaN absorption region and SiC multiplication region as a function of reverse bias for various densities of interface charge.

It can be shown that inequality (equation 6) requires

$$\varepsilon_{SiC} E_{SiC}^{cr} - \varepsilon_{GaN} E_{GaN}^{br} < \sigma_n < \varepsilon_{SiC} E_{SiC}^{cr} \tag{7}$$

It is important to note that $E_{GaN}{}^{br} << E_{SiC}{}^{cr}$ for heteroepitaxially grown GaN due to the presence of a large dislocation density at the hetero-interface that has been demonstrated to give rise to large leakage currents at low reverse bias in GaN p-n junction diodes. As a result, equation 7 indicates that the parameter space for optimal interface charge density, so that the detector can have both high QE and low dark current, is narrower in this case.

To appreciate the role of polarization-induced interface charge in practice, consider the specific case of a GaN/4H-SIC APD structure consisting of a 480-nm-thick n-type SiC multiplication region doped ~5 x 10^{15} cm^{-3} that has been demonstrated to yield low dark current SiC APDs (*2*), and a 300-nm-thick n-type GaN layer doped ~1 x 10^{16} cm^{-3} so as to have nearly full absorption above the bandgap of GaN in the absorption region for high QE. The net interface charge in this detector is calculated to be between ~0.013–0.023 C/m^2, using ~0.034 C/m^2 as the spontaneous polarization in GaN (*3*) and 0.011–0.021 C/m^2 for 4H-SiC, based upon the work of Bai et al. (*4*). The net interface charge may be excessive for the lower estimate of the spontaneous polarization for 4H-SiC, therefore preventing punch-through prior to avalanche breakdown in this detector (figure 2, right).

One approach to controlling the interface charge in this device is to employ strain engineering, since GaN is a piezoelectric material. Compressive strain in the GaN absorption region can reduce the net interface charge by inducing a piezoelectric charge with opposite sign to that of the spontaneous polarization charge, while tensile strain will increase the net interface charge. Figure 4 (top) shows the calculated electric field profile for the GaN/SiC SAM-APD biased just short of avalanche breakdown and assuming the GaN layer is compressively strained (–0.24). This strain state induces a piezoelectric charge that reduces the net interface charge to ~0.1 C/m^2, thus allowing punch-through prior to avalanche breakdown.

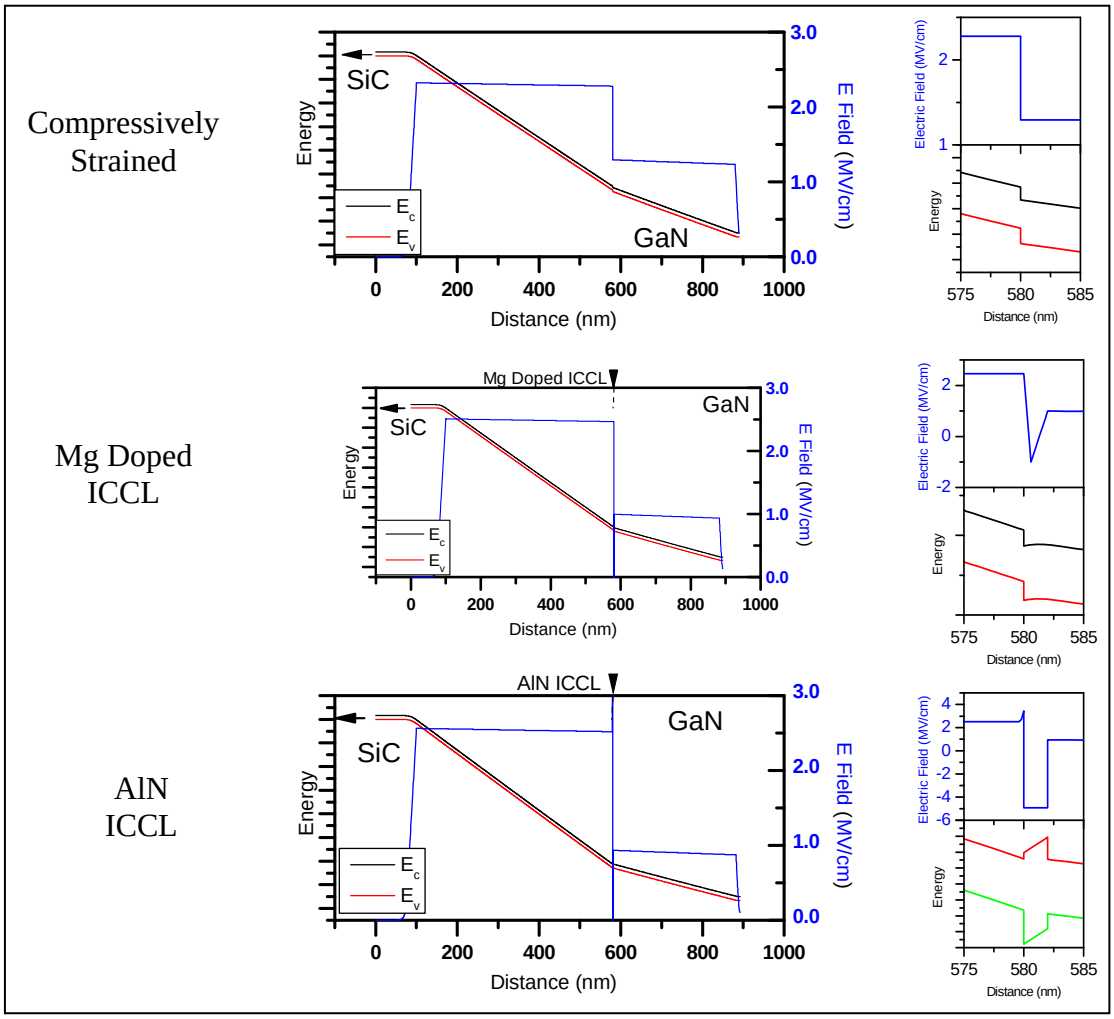

Figure 4. Calculation of the electric field and band diagram in a GaN/SiC SAM-APD accounting for spontaneous polarization charge for the case where the GaN layer is compressively strained (top), a p-type interface charge control layer (PICCL) is employed (middle), and an aluminum nitride (AlN) ICCL is employed (bottom). Exploded view of the hetero-interface for each case is shown to the right.

An alternative approach is to introduce charge at the interface through dopants. This ICCL can contain ionized acceptors or donors to provide negative or positive charge, respectively. To illustrate this concept, figure 4 (middle) shows the calculated electric field distribution in a GaN/SiC APD employing a 2-nm magnesium (Mg) doped PICCL at the hetero-interface that introduces a negative interface charge density of 0.11 C/m^2. This charge is sufficient to allow punch-through of the electric field into the GaN absorption region, but also introduces a small barrier for hole transport into the SiC multiplication region (figure 4, middle).

A third approach is to introduce a layer having larger spontaneous polarization than the absorption or multiplication region, for example, an AlN ICCL. This charge control layer introduces a type I band alignment between AlN and SiC that creates a 2DEG in the SiC multiplication region and a 2DHG in the GaN absorption region, as shown in figure 4 (bottom), with the effect of reducing the net interface charge density. However, the AlN ICCL also introduces a significant barrier for hole transport into the SiC multiplication region that may reduce carrier collection efficiency. This barrier may be reduced by employing an AlGaN ICCL having lower spontaneous polarization than AlN but still having sufficient bandgap energy so as to maintain a type-I band alignment and a dipole at the hetero-interface.

While SAM-APDs fabricated in other materials systems, such as InGaAs/InP SAM-APDs, require little electric field in the absorption region to achieve high QE because of large carrier diffusion lengths to collect carriers, GaN/SiC SAM-APDs likely cannot employ this approach due to the large density of dislocations that arise at hetero-interface resulting from lattice mismatch. In addition, since the interface between the SiC multiplication region and the GaN absorption region also coincides with the initiation of heteroepitaxial growth, the presence of surface impurities may act in concert with extended defects to further increase the probability of hole trapping at the interface and reduce detector QE. While dislocation densities as low as 10^8 cm^{-3} have been reported in GaN when employing a thin AlN buffer (*5*) or substrate patterning, these approaches may be undesirable due to the need for hole transport across the hetero-interface for collection. Instead, the presence of an electric field to decrease the transit time of photo-generated holes into the SiC multiplication region is likely essential to reduce the probability of trapping and obtain high QE.

The requirement for optimizing the net interface charge density to ensure a desirable low electric field in the III-Nitride absorption region should depend strongly upon the composition of the absorption region, which will affect both spontaneous and piezoelectric polarization. For the case of a GaN/SiC SAM-APD, residual tensile strain, which arises from the larger thermal expansion coefficient of GaN (5.59×10^{-6}/K) over that of SiC (~4.20×10^{-6}/K) despite the smaller *a* lattice constant of 4H-SiC (3.07 A) over GaN (3.18 A), should lead to an increase in σ_n over what would be expected for a fully relaxed structure. This strain can be managed by reducing the growth temperature or introducing an AlN buffer layer, which has been found to change the strain state in the GaN epilayer to compressive (*6*) and could, therefore, potentially provide an avenue for reducing the net interface charge. However, as discussed previously, the formation of

the 2DEG in the SiC that would also result in lower net interface charge density must also be taken into account so as to not increase the electric field in the GaN so much that dark current also increases. For a deep UV AlGaN/SAM-APD, the high AlN mole fraction absorption region will have larger spontaneous polarization that will likely result in an increase in net interface charge over a GaN/SiC SAM-APD, in conjunction with the reduction in strain due to the closer lattice match between AlN and 4H-SiC. While the spontaneous polarization component of the interface charge in InGaN/SiC SAM-APDs operating in the visible would likely be similar to that of a GaN/SiC SAM-APD, the piezoelectric component arising from tensile strain may be significantly higher in the former, depending upon the degree of relaxation that would occur. Thus, it is apparent that the use of an interface charge control layer provides an additional degree of control over the net charge density that allows for tailoring the electric field in the detector for optimal performance.

While this discussion treats the case of a GaN/SiC SAM-APD structure designed for the multiplication of holes, and therefore, employing a net positive interface charge, inverse arguments, including inversion of the crystal polarity to N-face, apply for a device designed for electron multiplication. In this case, the formation of a negative polarization charge is desirable. An important example of this case would be a III-N/Si (111) APD, which would require a p-type, N-polar III-Nitride contact layer and an unintentionally doped N-polar absorption region for efficient electron collection. Such devices are complicated by the observation that III-Nitride materials grown on Si (111) are reported to be III-polar as grown. More generally, these arguments can be applied to any SAM-APD structure composed of a multiplication and absorption region having unequal total polarization.

3.2 Devices

A series of GaN/SiC SAM-APDs were fabricated employing a 2-μm-thick p^+- SiC layer, a 480-nm-thick ν- SiC multiplication region, and a 300- to 500-nm-thick ν-GaN absorption region; and capped with a thin 10-nm-thick n^+-GaN layer so as to minimize absorption in this region. Figure 5 shows a scanning electron micrograph (SEM) of a typical fabricated APD employing a beveled sidewall to reduce the magnitude of the electric field along the circumference of the device with respect to the bulk so as to avoid premature breakdown. These devices are top illuminated through a silicon dioxide (SiO_2) passivation layer and electrically contacted using a titanium (Ti)/Al/nickel (Ni)/gold (Au) ohmic metal ring contact on the top n-GaN layer and a Ni/Ti/Al/Ni ohmic contact to the p-SiC layer (not visible in SEM image). These APDs exhibit dark currents as low as 0.1 nA near breakdown for a 130-μm-diameter device (figure 6, black curve) that is similar to what is observed for comparable SiC APDs (figure 6, green curve). This result suggests that the reverse leakage currents in these devices are limited by the SiC multiplication region despite the presence of threading dislocations at the hetero-interface. It is also important to note that the dark current in these devices is ~1000 times lower than what has been observed for GaN APDs despite having areas that are ~25 times larger.

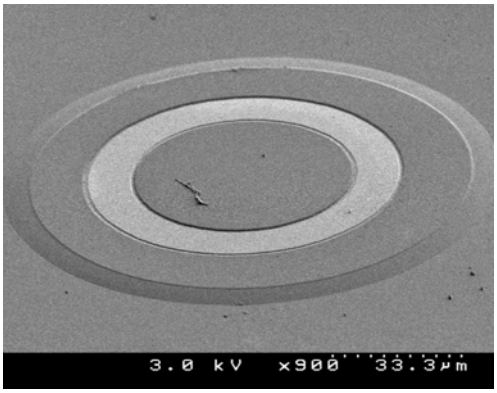

Figure 5. SEM micrograph of a fabricated GaN/SiC SAM-APD.

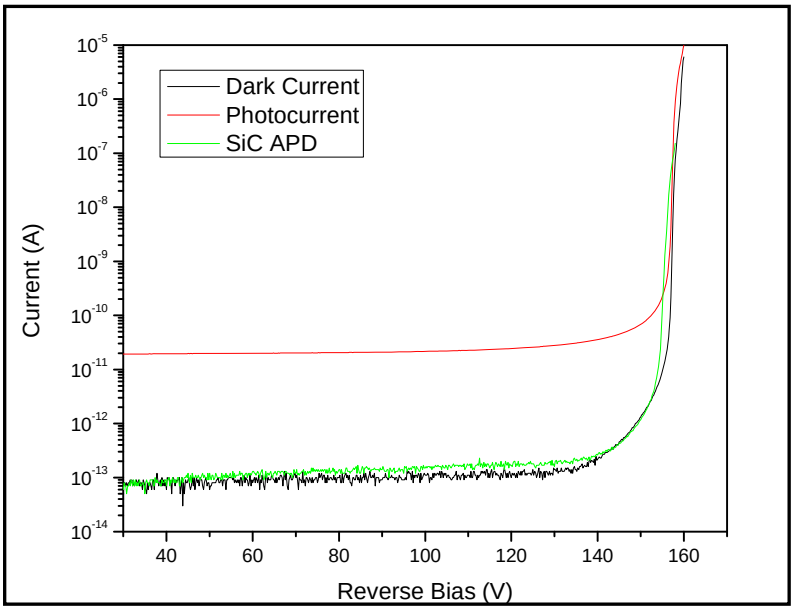

Figure 6. Measured dark current (blue) and photocurrent (red) for a 130-µm-diameter GaN/SiC APD. The dark current for a typical SiC APD is shown in green.

The photoresponse from these devices was measured using a Keithley 2410 source measurement unit to apply reverse bias and measure the current in the device under illumination and in the dark. The measured photoresponse from these initial devices was very weak with a peak QE of 0.25% at 354 nm and a response spectrum that was not consistent with the collection of photo-generated holes within the GaN absorption region (figure 7, left). Instead, the shape and intensity of the photoresponse in these devices can be explained by the absorption of photons within the SiC multiplication region that are not absorbed by the GaN absorption region. This is demonstrated by taking the product of the measured transmission through a 300-nm-thick GaN film and the measured spectral response of a SiC APD having a 480-nm-thick multiplication region (figure 7, right). This result is likely due to the predicted confinement of the electric field within the SiC multiplication region arising from excess polarization induced interface charge,

which leads to inefficient collection of photo-generated holes in the GaN absorption region arising from the confluence of (1) a reliance on the diffusion of photo-generated holes into the multiplication region and (2) the presence of a high density of defects at the hetero-interface that results in these carriers being lost to defect-mediated recombination.

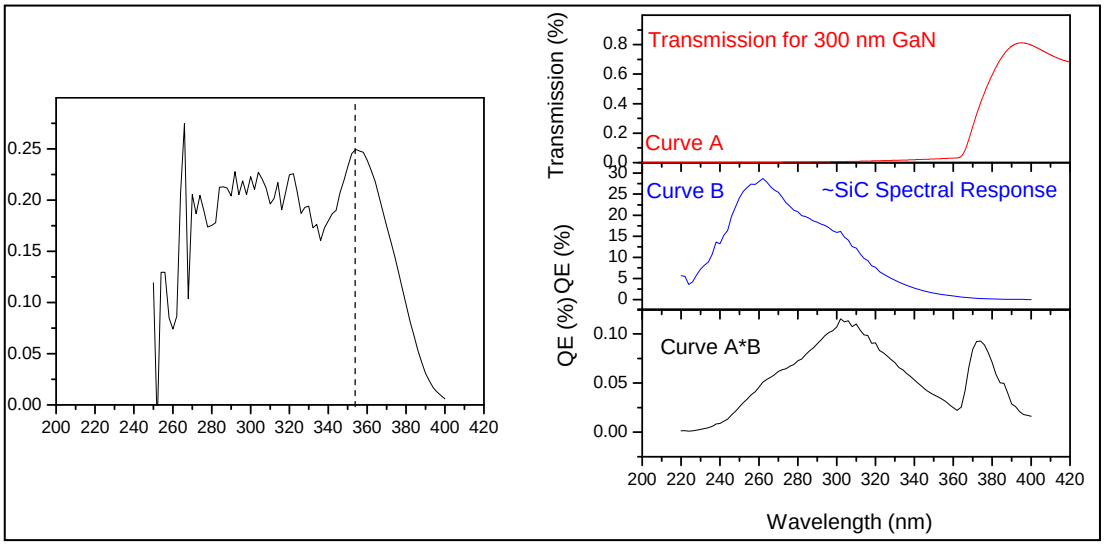

Figure 7. Measured spectral response for prototype GaN/SiC APD (left). Calculated spectral response for a SiC APD through the GaN absorption region (right, bottom) accounting for the transmission spectra for a typical GaN absorption region (right, top), and the spectral response for a SiC APD (right, middle).

A number of GaN/SiC APDs incorporating PICCLs of varying thicknesses were fabricated to optimize the total charge density at the hetero-interface as discussed in section 3.1. Figure 8 shows the measured responsivity at a reverse bias of 156 V for a number of APDs containing PICCLs with thickness varying from 2 to 15 nm so as to controllably increase the number of negative doping charges at the interface. The spectral response of the GaN/SiC SAM-APDs employing a 2.5- or 10-nm-thick Mg-doped interface layer (figure 8, black and blue curves) shows poor response dominated by the collection of carriers generated directly in the SiC multiplication region. In contrast, a GaN/SiC SAM-APD employing a 15-nm-thick Mg-doped GaN ICCL at the hetero-interface between the SiC substrate and the GaN absorption region exhibits strong GaN response with a peak responsivity of 40 mA/W (figure 8, red curve). This is attributed to the improvement in hole injection from the GaN absorption region due to the punch-through of the electric field into the GaN region with increased Mg doping in the interface layer. A peak responsivity of ~4.1 A/W was measured for these devices at a reverse bias of ~158 V.

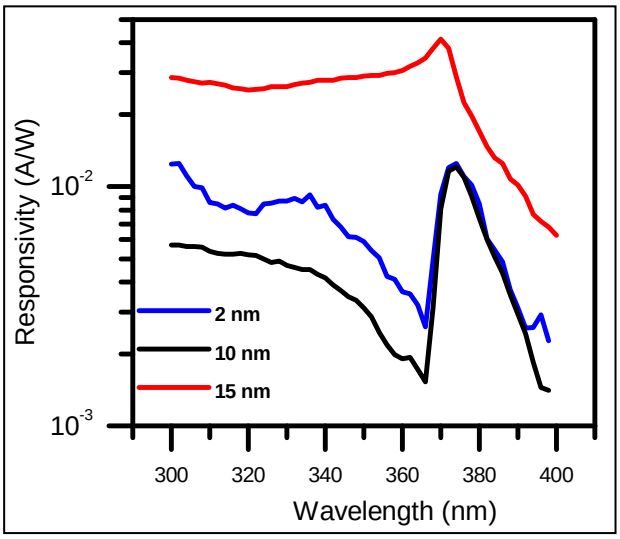

Figure. 8. Measured responsivity of GaN/SiC SAM-APDs employing p-type ICCLs with varying thicknesses.

4. Conclusions

III-Nitride/SiC SAM-APDs show great promise for realization of high gain detectors that can operate over a widely tunable spectrum in the near and deep UV, where there are currently limited alternatives. Prototype GaN/SiC SAM-APDs have been demonstrated that exhibit dark currents comparable to that of SiC APDs, and a peak responsivity of ~4 A/W. However, we have shown that the design and optimization of this device requires attention to the formation of interface charge that arises at the hetero-interface due to the difference in spontaneous polarization of 4H-SiC and GaN, as well as to the presence of defects at the interface. The former can determine the electric field profile in the detector, and the latter establishes the range of interface charge density that can simultaneously provide high QE with low dark current. The net interface charge density may be tailored to optimize device performance by employing strain management and/or introducing an interface charge control layer doped with acceptors or having larger spontaneous polarization.

5. References

1. Danielsson, E.; Zetterling, C.-M.; Ostling, M.; Linthicum, K.; Thompson, D. B.; Nam, O.-H.; Davis, R. F. The Influence of Band Offsets on the IV Characteristics for GaN/SiC Heterojunctions. *Sol. State Electron.* **2002**, *46*, 827–35.

2. Liu, M.; Bai, X.; Hu, C.; Guo, X.; Campbell, J. C.; Pan, Z.; Tashima, M. M. Low Dark Count Rate and High Single-photon Detection Efficiency Avalanche Photodiode in Geiger-mode Operation. *IEEE Phot. Tech. Lett.* **2007**, *19*, 378–80.

3. Vurgaftman, I. I.; Meyer, J. R. Band Parameters for Nitrogen-containing Semiconductors. *J. Appl. Phys.* **2003**, *94*, 3675–96.

4. Bai, S.; Devaty, R. P.; Choyke, W. J.; Kaiser, U.; Wagner, G.; MacMillan, M. F. Determination of the Electric Field in 4H/3C/4H-SiC Quantum Wells Due to Spontaneous Polarization in the 4H SiC Matrix. *Appl. Phys. Lett.* **2003**, *83*, 3171–3173.

5. Tanaka, S.; Iwai, S.; Aoyagi, Y. Reduction of the Defect Density in GaN Films Using Ultra-thin AlN Buffer Layers on 6H-SiC. *J. of Cryst. Growth* **1997**, *170*, 329–334 .

6. Perry, W. G.; Zheleva, T.; Bremser, M. D.; Davis, R. F.; Shan, W.; Song, J. J. Correlation of Biaxial Strains, Bound Exciton Energies, and Defect Microstructures in GaN Films Grown on AIN/6H-SiC(0001) Substrates. *J. of Electron Mat.* **1997**, *26*, 224–231.

6. Transitions

1. We contributed a paper to the 2010 Lester Eastman Conference on High Performance Devices (Troy, NY).
2. A manuscript entitled “III-Nitride/SiC Separate Absorption and Multiplication Avalanche Photodiodes: The Importance Of Controlling Polarization-Induced Interface Charge” has been has been accepted for publication in the *International Journal on High Speed Electronic Systems*.
3. Two provisional patent applications (61348141 entitled “Polar Semiconductor Photodetector with Transparent Interface and Method Thereof” and 61348959 entitled “Polarization Enhanced Substantially Separate Absorption and Multiplication Avalanche Photodiode System and Method Thereof”) have been filed with the U.S. Patent and Trademark Office based upon this work.

List of Symbols, Abbreviations, and Acronyms

2DEG	two-dimensional electron gas
AlN	aluminum nitride
APDs	avalanche photodiodes
Au	gold
ECBC	Edgewood Chemical and Biological Center
GaN	gallium nitride
ICCL	interface charge control layer
InGaAs	indium gallium arsenide
InGaN	indium gallium nitride
InP	indium phosphide
LCBAS	Low Cost Bioagent Sensor
Mg	magnesium
Ni	nickel
PICCL	p-type interface charge control layer
PMT	photomultiplier tube
QE	quantum efficiency
SAM-APDS	separate absorption and multiplication avalanche photodiodes
SEM	scanning electron micrograph
Si	silicon
SiC	silicon carbide
SiO_2	silicon dioxide
Ti	titanium
UV	ultraviolet

No. of Copies	Organization
1 ELEC	ADMNSTR DEFNS TECHL INFO CTR ATTN DTIC OCP 8725 JOHN J KINGMAN RD STE 0944 FT BELVOIR VA 22060-6218
2 ELEC	US ARMY RSRCH LAB ATTN RDRL SEE M A SAMPATH (anand.sampath@us.army.mil) M WRABACK (mwraback@arl.army.mil) 2800 POWDER MILL RD ADELPHI, MD 20783
1 CD	US ARMY RSRCH LAB ATTN RDRL CIM G T LANDFRIED BLDG 4600 ABERDEEN PROVING GROUND MD 21005-5066
3 CDS	US ARMY RSRCH LAB ATTN IMNE ALC HRR MAIL & RECORDS MGMT ATTN RDRL CIM L TECHL LIB ATTN RDRL CIM P TECHL PUB ADELPHI MD 20783-1197
TOTAL:	7 (3 ELEC, 4 CDS)

INTENTIONALLY LEFT BLANK.